Electronic states structure of Gd₅Sb₃ and Gd₅Ge₂Sb compounds according to band calculations and optical spectroscopy

© *Yu.V. Knyazev*[1], *A.V. Lukoyanov*[1,2,¶], *Yu.I. Kuz'min*[1], *S. Shanmukharao Samatham*[3],
Akhilesh Kumar Patel[4,5], *K.G. Suresh*[5]

[1] M.N. Mikheev Institute of Metal Physics, Ural Branch, Russian Academy of Sciences,
Yekaterinburg, Russia
[2] Ural Federal University after the first President of Russia B.N. Yeltsin,
Yekaterinburg, Russia
[3] Department of Physics, Chaitanya Bharathi Institute of Technology,
Gandipet, Hyderabad 500 075, India
[4] Department of Materials Science and Engineering, Faculty of Engineering, Tel Aviv University, Ramat Aviv,
Tel Aviv 6997801, Israel
[5] Magnetic Materials Laboratory, Department of Physics, Indian Institute of Technology Bombay,
Mumbai 400076, Maharashtra, India

¶ E-mail: lukoyanov@imp.uran.ru

Results of investigations of the electronic structure and optical properties of Gd₅Sb₃ and Gd₅Ge₂Sb compounds are presented. Calculations of band spectra were carried out in frame of local density approximation with a correction for strong correlation effects in $4f$ shell of rare-earth ion (DFT + U + SO method). Optical constants of these materials were measured by ellipsometric technique in wide wavelength interval. Energy dependencies of a number of spectral parameters were determined. The nature of quantum light absorption is discussed on the base of comparative analysis of the experimental and calculated spectra of optical conductivity.

1. Introduction

Binary intermetallic compounds R_5M_3 (where R — rare earth metal, $M-p$-element) crystallize in the hexagonal structure Mn₅Si₃-type, in which the unit cell consists of five layers of atoms in the direction of the c axis. To date, a large number of such materials have been synthesized and studied. The compounds of this series are characterized by a wide variety of magnetic properties, in particular, the presence of various magnetic phases, metamagnetic transitions, spin glass states, large magnetoresistive and magnetocaloric effects [1–13]. In this crystal structure, rare-earth metal ions are localized in two nonequivalent crystallographic positions that form different R-sublattices [14]. This circumstance leads to anisotropy of internal magnetic interactions, which is the reason for the formation of noncollinear magnetic structures, as well as to a complex behavior of the temperature dependences of magnetic and electronic parameters. The results of experimental studies indicate a strong interdependence of the magnetic, electronic, and structural characteristics of such materials. For a number of compounds of this series, calculations of the energy spectrum were carried out, in which the atomic magnetic moments were calculated and the nature of the electronic states near the Fermi level E_F [15–19] was determined. The electronic structure of some materials of this group has been studied experimentally by photoemission and optical spectroscopy [17–21].

In recent years, increased attention has been paid to the study of intermetallic compounds R_5M_3, where the rare earth element is gadolinium. Such interest is due to the fact that a giant magnetocaloric effect [22–24] was discovered in the Gd₅(Ge₄₋ₓSiₓ) alloy system similar in composition. The magnetic and electronic properties of binary Gd₅M_3 (M = Ge, Si, Bi, Sb) [25–30], as well as pseudobinary alloys, where p-elements are partially replaced by other metals [31–34] were investigated. This work is devoted to the study of the electronic structure and optical characteristics of Gd₅Sb₃ and Gd₅Ge₂Sb intermetallic compounds. A number of structural, electronic and magnetic parameters of these materials are presented in [30,34], where it is shown that below temperatures $T_N = 95.9$ K (Gd₅Sb) and $T_N = 136$ K (Gd₅Ge₂Sb) compounds are in the antiferromagnetic (AFM) state with noncollinear ordering of spin moments. The transition to the AFM phase is characterized by the appearance of strong anomalies in the temperature dependences of the magnetization, magnetic susceptibility, heat capacity, and electrical resistance.

2. Electronic structure calculation

The electronic structure of the intermetallic compounds Gd₅Sb₃ and Gd₅Ge₂Sb was modeled by the DFT + U + SO [35,36] method. This *ab initio* compu-

tational method combines the density functional theory (DFT) local density approximation with corrections for electron correlations $(+U)$ and spin-orbit coupling $(+SO)$ in a $4f$-shell of gadolinium ions. In this approach, the orbital basis included the atomic states $Gd(6s, 6p, 5d, 4f)$, Ge $(4s, 4p, 4d)$, and Sb $(5s, 5p, 5d)$. The following muffin-tin orbital radii were taken: $R_{Gd} = 3.7$ a.u., $R_{Ge} = 3.0$ a.u. and $R_{Sb} = 3.4$ a.u. To take into account the effects of electron-electron correlations, the values of U (Coulomb interaction parameter) equal to 6.7 eV and J (exchange interaction parameter) equal to 0.7 eV for Gd $4f$ were used. These U and J values are commonly used for Gd in intermetallic compounds, for example [37-39]. For sufficient convergence of the total energies, the accuracy 10^{-7} Ry was used. Integration in the reciprocal space was carried out over a grid with k points $10 \times 10 \times 10 = 1000$ using the tetrahedra method.

Figures 1 and 2 for the studied intermetallic compounds show the energy dependences of the total and partial densities of states $N(E)$ for $5d$-, $4f$-, $6s$- and $6p$-electrons Gd, $5s$- and $5p$-electrons Sb and $4s$-, $4p$-electrons Ge. Calculations showed that for both compounds in the range $-5 < E_F < 9$ eV the $N(E)$ spectrum consists of numerous maxima, the main contribution to the formation of which is related to $5d$- and $4f$-electrons Gd. The contributions to $N(E)$ from other partial densities are distributed unevenly over the entire energy range and are much weaker in magnitude. Intense bursts $N(E)$ of width ~ 1.5 eV observed in intervals $8-9.5$ eV below E_F and $1-3$ eV above E_F correspond to the partial densities of $4f$-electrons Gd in the filled and free bands. The metallic nature of the
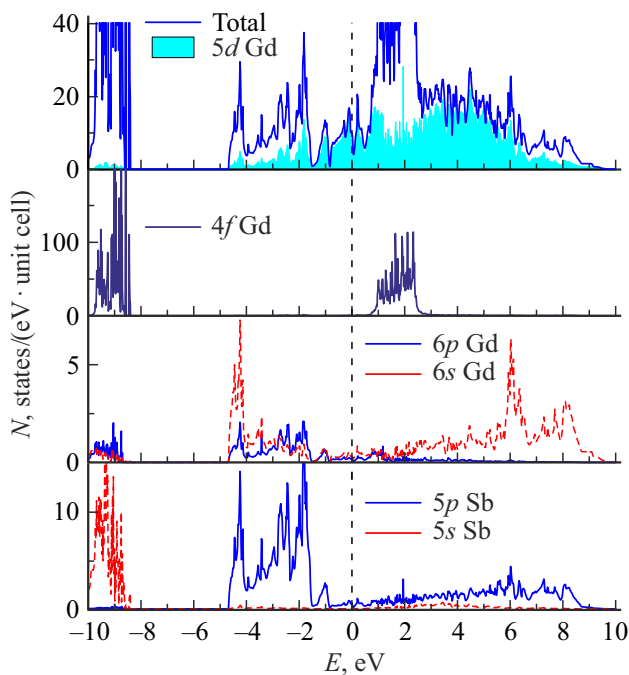

Figure 2. Total and partial densities of electronic states of the Gd_5Ge_2Sb compound.
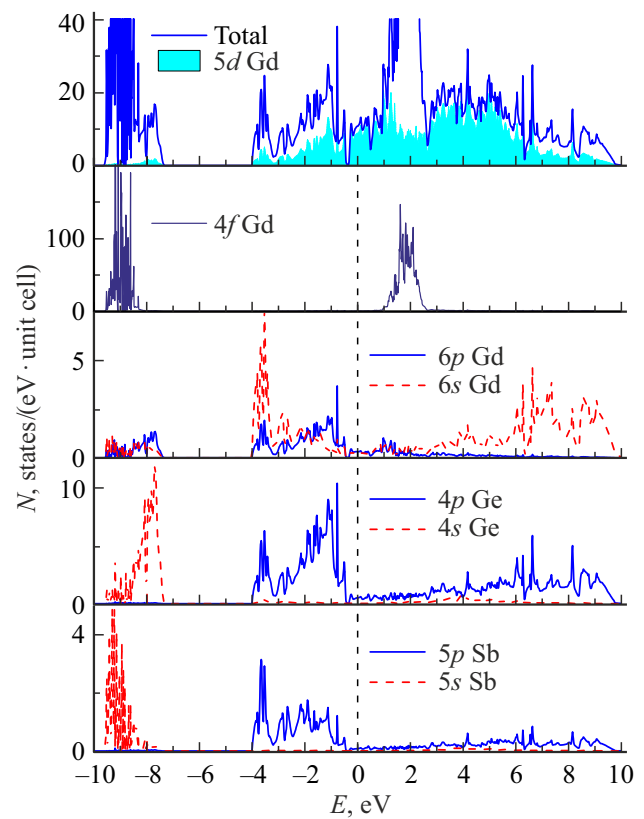
conductivity of the compounds is provided by the $5d$-states of gadolinium that reach the Fermi level. On the whole, the structural features of the energy dependences of the total densities of states for both alloys are quite similar. The observed differences are related to the changes introduced into the $N(E)$ ternary compound by contributions from $4s$- and $4p$-electrons Ge.

3. Experiment

The studied samples of Gd_5Sb_3 and Gd_5Ge_2Sb compounds were prepared by arc melting of stoichiometric proportions of high-purity metals (99.99%) in a pure argon atmosphere. The smelted ingots were annealed in vacuum for seven days at a temperature of $\sim 1000°C$ for the purpose of homogenization. X-ray diffraction analysis of powder samples was carried out on a PANalytical X'Pert PRO high-resolution diffractometer in CuK_α radiation. The study of the phase composition of the compounds and the calculation of the lattice parameters were performed on the basis of the FullProf program. The results of the analysis showed that both alloys crystallize in a single-phase hexagonal crystal structure of the Mg_5Si_3 type with lattice parameters $a = b = 9.02$Å, $c = 6.32$ Å (Gd_5Sb_3) and $a = b = 8.73$Å, $c = 6.40$ Å (Gd_5Ge_2Sb).

Figure 1. Total and partial densities of electronic states of the Gd_5Sb_3 compound.

The optical properties of the samples were studied in the wavelength range $\lambda = 0.22 - 13\,\mu$m $(0.095 - 5.64\,\text{eV})$, which includes the ultraviolet, visible, and infrared regions of the spectrum. Beatty's ellipsometric method, based on measuring the amplitudes and phase differences of the reflected light waves s- and p-polarizations, determined the optical constants of the compounds: the refractive indices $n(\lambda)$ and absorption coefficients $k(\lambda)$. The values of these parameters are used to calculate the dispersion dependences of a number of spectral functions characterizing the optical response of a reflecting medium — real $\varepsilon_1 = n^2 - k^2$ and imaginary $\varepsilon_2 = 2nk$ parts of the complex permittivity, reflectivity $R = [(n-1)^2 + k^2]/[(n+1)^2 + k^2]$, optical conductivity $\sigma = \varepsilon_2 \omega / 4\pi$ (ω — frequency of the light wave). The flat mirror surfaces of the samples corresponding to the 14th finish class (roughness $\sim 0.01\,\mu$m) were prepared by polishing on diamond pastes of various grain sizes. The penetration depth of light $\delta = c/k\omega$ (c — speed of light) in the investigated wavelength range increases from several tens (UV region) to several hundreds of atomic layers (IR region), which allows us to consider the obtained optical parameters as bulk characteristics of the materials under study.

4. Results and discussion

Wavelength dependences of the optical constants n and k for the Gd$_5$Sb$_3$ and Gd$_5$Ge$_2$Sb compounds are shown in Fig. 3 (the interval $\lambda < 2\,\mu$m is marked on the inset). With an increase λ, a significant increase in these values is observed, and the fulfillment of the relation $k > n$ over the entire range confirms the metallic nature of the conductivity of these materials. The nature of the change in the optical constants of both alloys is monotonic, except for the short-wavelength range, where there are a number of structures in the form of smoothed maxima. The dependences $\varepsilon_1(E)$ and $R(E)$ calculated from the values of n and k are shown in Fig. 4. The behavior of these characteristics is also typical for conducting media. This is manifested in the fact that the real part of the complex permittivity is negative at all energies of light quanta, and the reflectivity increases significantly with decreasing light frequency, reaching the value 0.9 at the low-energy edge of the interval.

The energy dependences of the optical conductivity $\sigma(E)$ are shown in Fig. 5 by dark circles. This parameter most expressively describes the frequency and amplitude features of the spectral response of the reflecting medium. In the spectral profile of these dependences, two regions are clearly manifested, corresponding to different mechanisms of electron photoexcitation — intraband and interband absorption of light. In the IR region at $E \lesssim 0.8\,\text{eV}$, the $\sigma(E)$ spectra of both compounds exhibit a sharp drop corresponding to Drude-type absorption ($\sigma \sim \omega^2$), at which the interaction of an electron with the field of a light wave occurs within the same energy band. In this frequency range, the interpretation of the optical properties
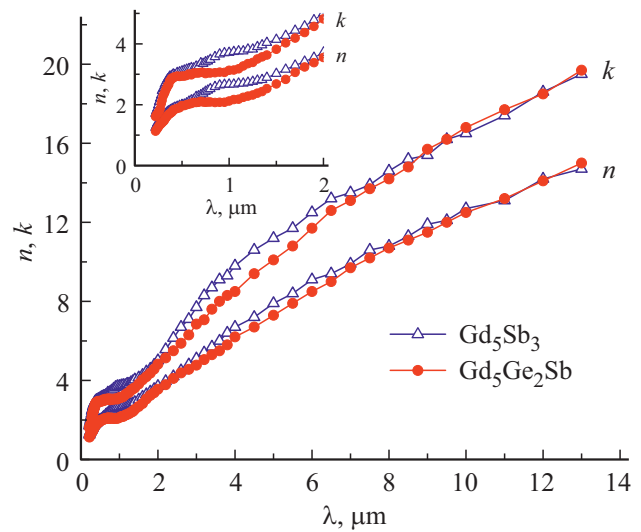

Figure 3. Dependences of the optical constants n and k of the Gd$_5$Sb$_3$ and Gd$_5$Ge$_2$Sb compounds on the wavelength of light incident on the sample. The short-wave interval is marked in the inset.
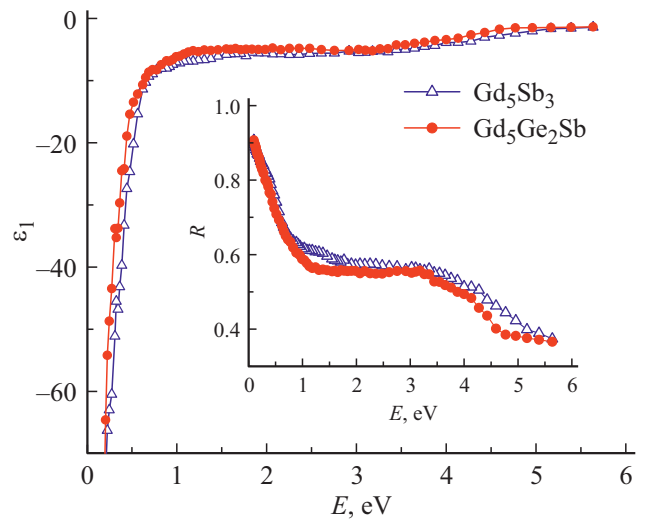

Figure 4. Energy dependences of the real part of permittivity and reflectivity (inset) of Gd$_5$Sb$_3$ and Gd$_5$Ge$_2$Sb compounds.

based on the equation of motion of an electron in an alternating electromagnetic field [40] allows one to calculate the plasma $\omega_P = [\omega^2(n^2+k^2)^2/(k^2-n^2)^2]^{1/2}$ and relaxation $\gamma = 2nk\omega/(k^2-n^2)$ carrier frequency. These parameters determine, respectively, the frequencies of collective oscillations and scattering of conduction electrons and take the values $\omega_P = 7.0 \cdot 10^{15}\,\text{s}^{-1}$, $\gamma = 5.1 \cdot 10^{14}\,\text{s}^{-1}$ (Gd$_5$Sb$_3$) and $\omega_P = 7.1 \cdot 10^{15}\,\text{s}^{-1}$, $\gamma = 5.3 \cdot 10^{14}\,\text{s}^{-1}$ (Gd$_5$Ge$_2$Sb). The relation $N = \omega_P^2 m/4\pi e^2$ makes it possible to calculate the conduction electron concentrations of the materials under study, which are close in magnitude and amount to $N \sim 8 \cdot 10^{22}\,\text{cm}^{-3}$. The resulting values of ω_P and γ, according to the expression $\sigma_D(E) = \omega_P^2 \gamma / 4\pi(\omega^2 + \gamma^2)$,
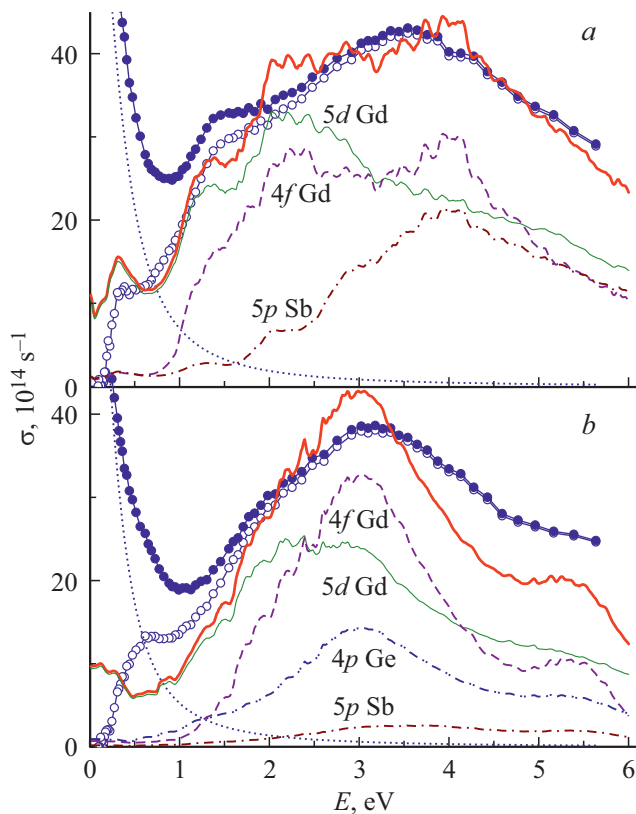
Figure 5. Optical conductivity spectra of Gd_5Sb_3 (a) and Gd_5Ge_2Sb (b) compounds Dark circles — experiment, light circles — interband contribution, solid lines calculation from total densities of states (in relative units). Dashed lines — intraband contribution. Also shown are the calculated contributions from interband transitions involving the Gd $4f$, $5d$, Sb $5p$, and Ge $4p$ electronic states.

make it possible to isolate the Drude contribution to the optical conductivity of each compound. The corresponding energy dependences $\sigma_D(E)$ are shown for both intermetallic compounds by dotted line. At $E \lesssim 2\,eV$ the intraband and interband contributions to the optical conductivity coexist, and above this energy the role of the intraband mechanism of light absorption becomes practically insignificant.

A fundamentally different behavior of the $\sigma(E)$ dependences is observed in the energy range above $E \gtrsim 1\,eV$ (visible and UV regions). In this range, the mechanism of quantum absorption of light dominates, due to the transitions of electrons from occupied states to free states. This mechanism is associated with the emergence of a number of features, the shape of which is individual for each material and is determined by its electronic structure. The $\sigma(E)$ spectra of the compounds under study in this range also differ significantly: if the broad absorption band in Gd_5Sb_3 is characterized by two maxima (near 1.5 and 3.5 eV), then in the corresponding dependence for Gd_5Ge_2Sb there is one maximum at $\sim 3\,eV$. The contributions of the interband absorption $\sigma_{inter}(E)$ to the optical conductivity of each intermetallic compound (light circles in Fig. 5) are

separated by subtracting the intraband components from the experimental dependences $\sigma_{inter}(E) = \sigma(E) - \sigma_D(E)$.

The main feature of the $\sigma_{inter}(E)$ spectra in these compounds is a high level of interband absorption in almost the entire energy range under study. To understand its nature, it makes sense to compare the experimental dependences $\sigma_{inter}(E)$ with the theoretical curves obtained from the densities of electronic states (Figs 1 and 2). Such a comparison is shown in Fig. 5, where the calculated interband conductivities are shown by continuous lines. The calculations were carried out in accordance with the [41] method based on convolutions of the total densities of states below and above the Fermi level. In view of the qualitative nature of the calculation, performed under the condition of equal probability of all types of electronic transitions, these dependences are presented in relative units. The structure of these curves, in general, quite well reproduces the nature of the dispersion of empirical dependences, as well as the localization and extent of the main features, although a complete correlation is not observed in small details. Figure 5 also shows calculations of the most significant partial contributions to $\sigma_{inter}(E)$ associated with various electronic states. As the figure shows, the dominant contributions in both compounds are formed by quantum transitions involving $5d$- and $4f$-electrons Gd. In Gd_5Sb_3, a significant contribution to interband optical absorption is made by transitions that capture $5p$-electrons Sb, while in Gd_5Ge_2Sb — $4p$-electrons Ge. Absorption involving other types of interband transitions is much weaker and is not shown in the figure. Thus, the comparison made shows that the intense interband absorption in the materials under study is of a similar nature. On the whole, the qualitative similarity of the spectral profile of the experimental and theoretical $\sigma_{inter}(E)$ dependences indicates that the calculations of the electronic structure give an adequate description of the optical properties of these compounds.

5. Conclusion

The paper presents the results of $LDA + U + SO$ calculations of the electronic structure of Gd_5Sb_3 and Gd_5Ge_2Sb intermetallic compounds. Calculations have shown that the total density of electronic states near the Fermi level is determined mainly by $5d$- and $4f$-states Gd, and the contributions associated with s- and p-states Sb and Ge have a much smaller value. The ellipsometry method was used to study the optical properties of these materials in the wavelength range $0.22-13\,\mu m$. Based on the calculated densities of electronic states, the nature of interband absorption and the appearance of the main structural features of the optical conductivity spectra are interpreted. The calculated energy dependences $\sigma_{inter}(E)$ qualitatively reproduce the shape of the experimental curves. From the values of optical constants measured in the infrared region of the spectrum, the plasma and relaxation frequencies of conduction electrons are determined.

Funding

Conflict of interest

The authors declare that they have no conflict of interest.

References

[1] J. Roger, M. Ben Yahia, V. Babizhetskyy, J. Bauer, S. Cordier, R. Guérin, K. Hiebl, X. Rocquefelte, J.-Y. Saillard, J.-F. Halet. J. Solid State Chem. **179**, *8*, 2310 (2006).

[2] T. Tsutaoka, Y. Nishiume, T. Tokunaga. JMMM **272–276**, e421 (2004).

[3] T. Tsutaoka, A. Tanaka, Y. Narumi, M. Iwaki, K. Kindo. Physica B: Condens. Matter **405**, *1*, 180 (2010).

[4] D.A. Joshi, A. Thamizhavel, S.K. Dhar. Phys. Rev. B **79**, *1*, 014425 (2009).

[5] B. Maji, K.G. Suresh, A.K. Nigam. J. Phys.: Condens. Matter **23**, *50*, 506002 (2011).

[6] R. Nirmala, A.V. Morozkin, A.K. Nigam, J. Lamsal, W.B. Yelon, O. Isnard, S.A. Granovsky, K.K. Bharathi, S. Quezado, S.K. Malik. J. Appl. Phys. **109**, *7*, 07A716 (2011).

[7] A.V. Morozkin, O. Isnard, P. Henry, P. Manfrinetti. JMMM **307**, *1*, 124 (2006).

[8] A.V. Morozkin, O. Isnard, P. Henry, P. Manfrinetti. J. Alloys Compd. **464**, 219 (2008).

[9] G. Tian, H. Du, Y. Zhang, Y. Xia, C. Wang, J. Han, S. Liu, J. Yang. J. Appl. Phys. **107**, *9*, 09A917 (2010).

[10] N. Mohapatra, K. Mukherjee, K.K. Iyer, E.V. Sampathkumaran. J. Phys.: Condens. Matter **23**, *49*, 496001 (2011).

[11] M. Falkowski, A. Kowalczyk, T. Toliński. JMMM **331**, 144 (2013).

[12] S.N. Jammalamadaka, N. Mohapatra, S.D. Das, E.V. Sampathkumaran. Phys. Rev. B **79**, *6*, 060403 (2009).

[13] B. Maji, K.G. Suresh, A.K. Nigam. Europhis. Lett. **91**, *3*, 37007 (2010).

[14] N. Mohapatra, S.D. Das, K. Mukherjee, K.K. Iyer, E.V. Sampathkumaran. Phys. Rev. B **80**, *21*, 214425 (2009).

[15] M. Djermouni, M. Belhadj, S. Kacimi, A. Zaoui. Mod. Phys. Lett. B **25**, *32*, 2427 (2011).

[16] N.A. Zabidi, H.A. Kassim, K.N. Shrivastava. AIP Conf. Proc. **1325**, *1*, 198 (2010).

[17] Yu.V. Knyazev, A.V. Lukoyanov, Yu.I. Kuz'min, B. Maji, K.G.Suresh. J. Alloys Compd. **588**, 725 (2014).

[18] Yu.V. Knyazev, A.V. Lukoyanov, Yu.I. Kuz'min. Physics of the Solid State **56**, *9*, 1737 (2014).

[19] Yu.V. Knyazev, A.V. Lukoyanov, Yu.I. Kuz'min. Physica B: Condens. Matter **442**, 12 (2014).

[20] L. Braicovich, E. Puppin, I. Lindau, A. Iandelli, G.L. Olcese, A. Palenzona. Phys. Rev. B **41**, *5*, 3123 (1990).

[21] C. Chemelli, S. Luridiana, M. Sancrotti, L. Braicovich, F. Ciccacci, A. Iandelli, G.L. Olcese, A. Palenzona. Phys. Rev. B **42**, *3*, 1829 (1990).

[22] V.K. Pecharsky, K.A. Gschneidner Jr. Phys. Rev. Lett. **78**, *23*, 4494 (1997).

[23] K.A. Gschneidner Jr., V.K. Pecharsky, A.O. Tsokol. Rep. Prog. Phys. **68**, *6*, 1479 (2005).

[24] V.K. Pecharsky, A.P. Holm, K.A. Gschneidner Jr., R. Rink. Phys. Rev. Lett. **91**, *19*, 197204 (2003).

[25] P. Kushwaha, R. Rawat. Solid State Commun. **152**, *19*, 1824 (2012).

[26] M. Nagai, A. Tanaka, Y. Haga, T. Tsutaoka. JMMM **310**, *2*, 1775 (2007).

[27] J.M. Cadogan, D.H. Ryan, Ya. Mudryk, V.K. Pecharsky, K.A. Gschneidner Jr. J. Appl. Phys. **115**, *17*, 17A901 (2014).

[28] F. Canepa, S. Cirafici, M. Napoletano. J. Alloys Compd. **335**, L1 (2002).

[29] Yu.V. Knyazev, A.V. Lukoyanov, Yu.I. Kuzmin. FTT **59**, *3*, 419 (2017).

[30] S.S. Samatham, A.K. Patel, A.V. Lukoyanov, K.G. Suresh. J. Phys.: Condens. Matter **30**, *29*, 295802 (2018).

[31] V. Svitlyk, F. Fei, Y. Mozharivskyj. J. Solid State Chem. **181**, *5*, 1080 (2008).

[32] T. Zhang, Y. Chen, Y. Tang, M. Tu. J. Alloys Compd. **422**, *1–2*, 25 (2006).

[33] E. Yüzüak, I. Dincer, Y. Elerman. J. Rare Earths **28**, *3*, 477 (2010).

[34] S.S. Samatham, A.K. Patel, A.V. Lukoyanov, K.G. Suresh. J. Alloys Compd. **806**, 575 (2019).

[35] A.O. Shorikov, A.V. Lukoyanov, M.A. Korotin, V.I. Anisimov. Phys. Rev. B **72**, *2*, 024458 (2005).

[36] H.-J. Lee, Y.-N. Choi, A.V. Lukoyanov, E.G. Gerasimov, A.N. Pirogov. JMMM **475**, 593 (2019).

[37] S. Gupta, K.G. Suresh, A.V. Lukoyanov. J. Mater. Sci. **50**, 5723 (2015).

[38] Yu.V. Knyazev, A.V. Lukoyanov, Yu.I. Kuz'min, V.S. Gaviko. Low Temperature Physics **44**, *2*, 157 (2018).

[39] F. Guillou, A.K. Pathak, T.A. Hackett, D. Paudyal, Y. Mudryk, V.K. Pecharsky. J. Phys.: Condens. Matter **29**, *48*, 485802 (2017).

[40] A.V. Sokolov. Optical properties of metals. State Publishing House of Physical and Mathematical Literature/Moscow (GIMFL) (1961). 464 p. (in Russian).

[41] I.I. Mazin, D.J. Singh, C. Ambrosch-Draxl. Phys. Rev. B **59**, *1*, 411 (1999).